

Iron, Ruthenium, and Osmium Complexes Supported by the Bis(silyl) Chelate Ligand (9,9-Dimethylxanthene-4,5-diyl)bis(dimethylsilyl): Synthesis, Characterization, and Reactivity

Jim Josephus G. Minglana,[†] Masaaki Okazaki,[‡] Kenji Hasegawa, Lung-Shiang Luh, Nobukazu Yamahira, Takashi Komuro, Hiroshi Ogino,[§] and Hiromi Tobita*

Department of Chemistry, Graduate School of Science, Tohoku University, Sendai 980-8578, Japan

Received July 19, 2007

The bis(silyl)-type bidentate ligand precursors xantsil-H₂ (**1a**) and 2,7-di-*t*-butylxantsil-H₂ (**1b**) possessing the xanthene backbone were prepared by dilithiation of the 4,5-positions of 9,9-dimethylxanthene or 2,7-di-*t*-butyl-9,9-dimethylxanthene using *n*-BuLi in the presence of tetramethylethylenediamine (TMEDA) followed by treatment with chlorodimethylsilane. According to X-ray diffraction analysis of **1b**, the xanthene core is close to planar as observed in the dihedral angle of 6.2(2)^o between two least-square planes of two aromatic rings in xanthene. UV irradiation of [Fe(CO)₅] and **1a** in dichloromethane provided *cis*-[Fe(xantsil)(CO)₄] (**2**), while thermal reactions of [M₃(CO)₁₂] (M = Ru and Os) and **1a** provided *cis*-[M(xantsil)(CO)₄] (M = Ru (**3**) and Os (**4**)). In the course of the synthetic study on **3**, formation of [Ru₃(xantsil)(μ-H)₂(CO)₁₀] (**5**) was confirmed and independently synthesized by the reaction of [Ru₃(CO)₁₀(CH₃CN)₂] with **1a**. Thermolysis of **5** and **1a** at 120 °C for 13 min afforded **3**, indicating its intermediacy to **3**. Refluxing the toluene solution of **3** for 3 h resulted in the replacement of three carbonyl ligands with toluene to give [Ru(xantsil)(CO)(η⁶-toluene)] (**6**). Dissociation of the three carbonyl ligands would be enhanced by the severe steric repulsion between the SiMe₂ moiety and the three fac-carbonyl ligands, high trans effect of silyl groups, and precoordination of the xanthene oxygen atom.

Introduction

The design and fine-tuning of ancillary ligands are important in the development of new transition-metal-catalyzed reactions. Diphosphines (abbreviated to P[∧]P), for example, have been shown to influence the reactivity and selectivity of metal centers in a manner dependent on the bite angle.¹ In Pt(P[∧]P) systems, the reactivity toward activation of C–H and C–X bonds increases with decreasing the P–Pt–P angle,² while in the [Pt(H)(C₂H₄)(P[∧]P)]⁺ systems, the introduction of diphosphines with a large bite angle accelerates the insertion of ethylene into the Pt–H bond, consistent with the predicted transition state for a widened P–Pt–P angle.³ High regioselectivity in the rhodium-catalyzed hydroformylation of 1-alkenes can be achieved by introducing diphosphines with a large bite angle.⁴ Several diphosphine ligands with a variety of xanthene-type backbones (xantphos) have been developed, and the beneficial

effects on catalytic activity and selectivity based on the rigidity of the xanthene core and the large bite angle have been demonstrated (Chart 1).^{1,5} We are now applying this unique backbone of xanthene to the bis(silyl)-type bidentate ligand, (9,9-dimethylxanthene-4,5-diyl)bis(dimethylsilyl), or “xantsil” (Chart 1).

Complexation of a silyl silicon atom with a transition-metal center has a marked effect on the properties of the metal complex, attributable to the exceptionally strong σ-donor character and high trans influencing character of the silyl group.⁶ Silyl groups are thus expected to be useful as ancillary ligands suitable for preparing coordinatively unsaturated, electron-rich

* Corresponding author. E-mail: tobita@mail.tains.tohoku.ac.jp.

[†] Institute of Chemistry, University of the Philippines, Diliman, Quezon City 1101, Philippines.

[‡] International Research Centre for Elements Science, Institute for Chemical Research, Kyoto University, Uji Kyoto, 611-0011, Japan.

[§] The Open University of Japan, Chiba, 261-8586, Japan.

(1) (a) van Leeuwen, P. W. N. M.; Kamer, P. C. J.; Reek, J. N. H.; Dierkes, P. *Chem. Rev.* **2000**, *100*, 2741. (b) Kamer, P. C. J.; van Leeuwen, P. W. N. M.; Reek, J. N. H. *Acc. Chem. Res.* **2001**, *34*, 895. (c) Freixa, Z.; van Leeuwen, P. W. N. M. *Dalton Trans.* **2003**, 1890. (d) Zuidema, E.; van Leeuwen, P. W. N. M.; Bo, C. *Organometallics* **2005**, *24*, 3703.

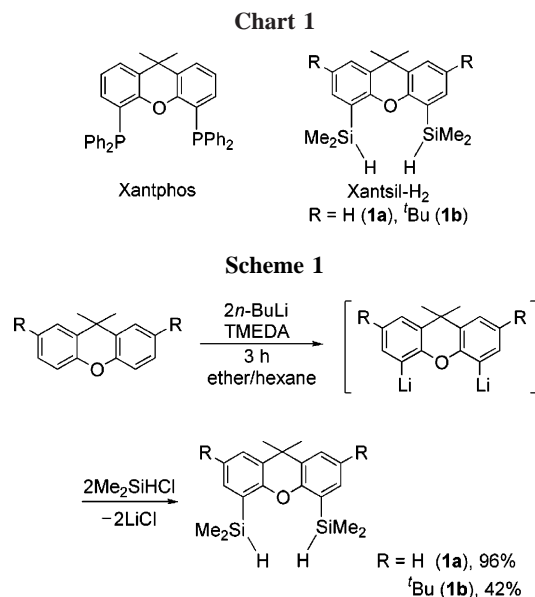
(2) Hofmann, P.; Heiss, H.; Neiteler, P.; Müller, G.; Lachmann, J. *Angew. Chem., Int. Ed. Engl.* **1990**, *29*, 880.

(3) (a) Thorn, D. L.; Hoffmann, R. *J. Am. Chem. Soc.* **1978**, *100*, 2079. (b) Coussens, B. B.; Buda, F.; Oevering, H.; Meier, R. J. *Organometallics* **1998**, *17*, 795.

(4) Casey, C. P.; Whiteker, G. T.; Melville, M. G.; Petrovich, L. M.; Gavney, J.; Powell, D. R. *J. Am. Chem. Soc.* **1992**, *114*, 5535.

(5) Kranenburg, M.; van der Burgt, Y. E. M.; Kamer, P. C. J.; van Leeuwen, P. W. N. M. *Organometallics* **1995**, *14*, 3081. (b) Kranenburg, M.; Delis, J. G. P.; Kamer, P. C. J.; van Leeuwen, P. W. N. M.; Vrieze, K.; Veldman, N.; Spek, A. L.; Goubitz, K.; Fraanje, J. *J. Chem. Soc., Dalton Trans.* **1997**, 1839. (c) Buhling, A.; Kamer, C. J.; van Leeuwen, P. W. N. M.; Elgersma, J. W.; Goubitz, K.; Fraanje, J. *Organometallics* **1997**, *16*, 3027. (d) Kranenburg, M.; Kamer, P. C. J.; van Leeuwen, P. W. N. M. *Eur. J. Inorg. Chem.* **1998**, 155. (e) Goedheijt, M. S.; Reek, J. N. H.; Kamer, P. C. J.; van Leeuwen, P. W. N. M. *Chem. Commun.* **1998**, 2431. (f) Goertz, W.; Keim, W.; Vogt, D.; Englert, U.; Boele, M. D. K.; van der Veen, L. A.; Kamer, P. C. J.; van Leeuwen, P. W. N. M. *J. Chem. Soc., Dalton Trans.* **1998**, 2981. (g) van der Veen, L. A.; Boele, M. D. K.; Bregman, F. R.; Kamer, P. C. J.; van Leeuwen, P. W. N. M.; Goubitz, K.; Fraanje, J.; Schenk, H.; Bo, C. *J. Am. Chem. Soc.* **1998**, *120*, 11616.

(6) (a) Chatt, J.; Eaborn, C.; Ibeke, S. *Chem. Commun.* **1966**, 700. (b) McWeeny, R.; Mason, R.; Towl, A. D. C. *Discuss. Faraday Soc.* **1969**, *47*, 20. (c) Chatt, J.; Eaborn, C.; Ibeke, S. D.; Kapoor, P. N. *J. Chem. Soc. A* **1970**, 1343. (d) Bentham, J. E.; Cradock, S.; Ebsworth, E. A. V. *J. Chem. Soc. A* **1971**, 587. (e) Hartley, F. R. *Chem. Soc. Rev.* **1973**, *2*, 163. (f) Haszeldine, R. N.; Parish, R. V.; Setchfield, J. H. *J. Organomet. Chem.* **1973**, *57*, 279. (g) Yamashita, H.; Hayashi, T.; Kobayashi, T.; Tanaka, M.; Goto, M. *J. Am. Chem. Soc.* **1988**, *110*, 4417. (h) Lichtenberger, D. L.; Rai-Chaudhuri, A. *J. Am. Chem. Soc.* **1991**, *113*, 2923. (i) Levy, C. J.; Puddephatt, R. J.; Vittal, J. J. *Organometallics* **1994**, *13*, 1559. (j) Brost, R. D.; Bruce, G. C.; Joslin, F. L.; Stobart, S. R. *Organometallics* **1997**, *16*, 5669.



metal centers. However, the facile cleavage of metal–silicon bonds via reductive elimination, nucleophilic attack at the silicon atom, insertion, or σ -bond metathesis,⁷ have obstructed progress in this area.⁸ The xantsil ligand with the xanthene backbone is expected to prevent reactions that lead to such cleavage of the metal–silicon bonds. In the present paper, the ligand precursor xantsil-H₂ (**1**) is synthesized and characterized by spectroscopy and X-ray diffraction analyses. The coordination of xantsil with group-8 transition metals in κ^2Si_2Si fashion can be achieved through the reactions of [Fe(CO)₅] or [M₃(CO)₁₂] (M = Ru, Os) with **1a** under photochemical or thermal conditions. The nature of the bis(silyl) ancillary ligand with the xanthene core is discussed based on the crystal structures, dynamic behavior in solution, and reactivity of the metal complexes. Part of this work has been published previously in a preliminary form.⁹

Results and Discussion

The ligand precursors **1a** and **1b** were prepared by dilithiation of the 4,5-positions of 9,9-dimethylxanthene or 2,7-di-*t*-butyl-9,9-dimethylxanthene using *n*-BuLi in the presence of tetramethylethylenediamine (TMEDA) followed by treatment with dimethylchlorosilane (Scheme 1). Analytically pure samples of **1a** (96%) and **1b** (42%) were obtained by subjecting the reaction mixtures to silica-gel flash chromatography. In the ¹H NMR spectrum of **1a**, the signal of SiMe₂ appears at δ 0.43 as a doublet coupled with the septet signal of SiH at δ 5.15 ($J = 3.5$ Hz). The ²⁹Si{¹H} NMR spectrum of **1a** contains a resonance at δ -22.2, the chemical shift characteristic of

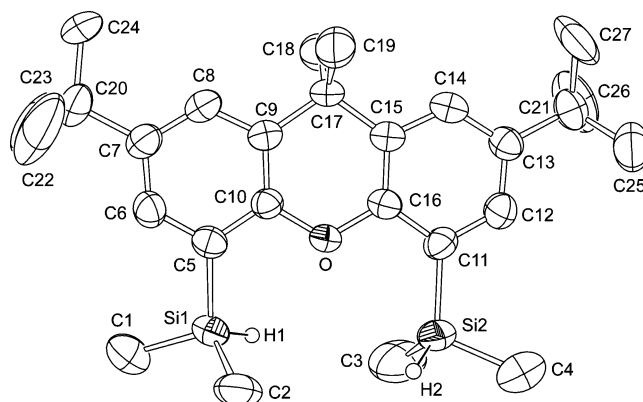
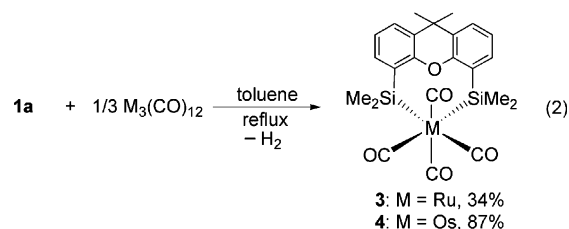
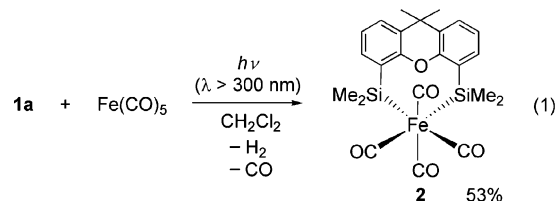


Figure 1. ORTEP drawing of **1b**. Thermal ellipsoids are drawn at the 50% probability level.

monohydrosilanes. The spectroscopic features of **1b** closely resemble those of **1a**.

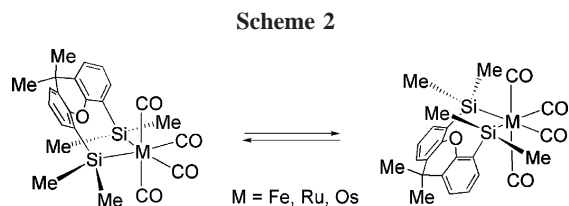
Single crystals of **1b** suitable for X-ray diffraction analysis were obtained by recrystallization from hot hexane. The molecular structure of **1b** is shown in Figure 1. The molecule has a pseudo-C₂ axis of symmetry through O and C17. The xanthene core is close to planar, as indicated by the small dihedral angle (6.2(2)°) between the two least-square planes of the two aromatic rings. The interatomic distance between Si1 and Si2 is 4.624(2) Å.

Ultraviolet irradiation ($\lambda > 300$ nm) of [Fe(CO)₅] and **1a** in dichloromethane provided *cis*-[Fe(xantsil)(CO)₄] (**2**) as the main product, which was purified by silica-gel flash chromatography (eq 1). Slow evaporation of the eluent afforded colorless crystals of **2** in 53% yield. The synthesis of **2** using [Fe(CO)₅] or [Fe₂(CO)₉] under thermal conditions was not successful due to the thermal instability of the resulting Fe(II) complexes. The ruthenium and osmium analogues, however, were obtainable under thermal conditions. Refluxing the toluene solutions of [M₃(CO)₁₂] and 3 equiv of **1a** resulted in the formation of *cis*-[M(xantsil)(CO)₄] (M = Ru (**3**), 34%; Os (**4**), 87%) as colorless crystals (eq 2). The low isolated yield of **3** is attributable to the further reaction of **3** with toluene (vide infra).



All three complexes exhibit similar NMR and IR spectroscopic features. In the IR spectra, four intense ν_{CO} bands are apparent in the region of 1981–2100 cm⁻¹, consistent with the *cis*-ML₂(CO)₄ geometry of C_{2v} symmetry. The ²⁹Si{¹H} NMR spectra display resonances at δ 9.0 (**2**), -8.2 (**3**), and

(7) (a) Tilley, T. D. In *The Chemistry of Organic Silicon Compounds*; Patai, S., Rappoport, Z., Eds.; Wiley: New York, 1989; Chapter 24, p 1415. (b) Tilley, T. D. In *The Silicon-Heteroatom Bond*; Patai, S., Rappoport, Z., Eds.; Wiley: New York, 1991; Chapters 9 and 10, pp 245 and 309. (c) Eisen, M. S. In *The Chemistry of Organic Silicon Compounds*; Rappoport, Z., Apeloig, Y., Eds.; Wiley: New York, 1998; Vol. 2, Chapter 35, p 2037. (d) Corey, J. Y.; Braddock-Wilking, J. *Chem. Rev.* **1999**, *90*, 175. (e) Okazaki, M.; Tobita, H.; Ogino, H. *Dalton Trans.* **2003**, 493. (8) (a) Brost, R. D.; Bruce, G. C.; Joslin, F. L.; Stobart, S. R. *Organometallics* **1997**, *16*, 5669. (b) Stobart, S. R.; Zhou, X.; Cea-Olivares, R.; Toscano, A. *Organometallics* **2001**, *20*, 4766. (c) Okazaki, M.; Tobita, H.; Ogino, H. *J. Chem. Soc., Dalton Trans.* **1997**, 3531. (d) Okazaki, M.; Tobita, H.; Kawano, Y.; Inomata, S.; Ogino, H. *J. Organomet. Chem.* **1998**, *553*, 1. (e) Okazaki, M.; Ohshitanai, S.; Tobita, H.; Ogino, H. *Chem. Lett.* **2001**, 952. (f) Okazaki, M.; Ohshitanai, S.; Tobita, H.; Ogino, H. *Coord. Chem. Rev.* **2002**, *226*, 167 and references therein. (9) Tobita, H.; Hasegawa, K.; Minglana, J. J. G.; Luh, L.-S.; Okazaki, M.; Ogino, H. *Organometallics* **1999**, *18*, 2058.



−31.7 (4). The trend is similar to that found for the group 8 metal complexes of *cis*-[M(SiMe₃)₂(CO)₄] (M = Fe (δ 26.6), Ru (δ 2.1), and Os (δ −22.8)).¹⁰ At room temperature, each of the ¹H NMR signals of the SiMe and 9-CMe groups on xantsil produces one singlet signal, indicating the existence of fluxional behavior. Inversion of the puckered chelate ring is likely, as shown in Scheme 2.⁹

The structures of **2**, **3**, and **4** were unequivocally determined by X-ray crystal structure analysis (Figures 2–4). Selected interatomic distances and angles are listed in Table 1. The two mutually *cis*-silyl groups and four carbonyl ligands adopt a distorted octahedral arrangement around the metal center. The bite angles of Si–M–Si (94.9–97.5°) are widened slightly from

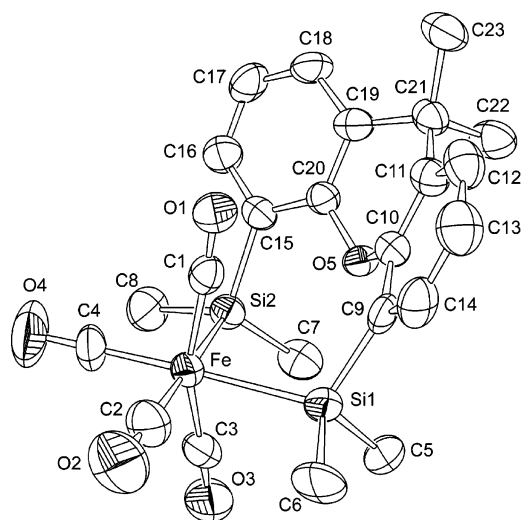


Figure 2. ORTEP drawing of *cis*-[Fe(xantsil)(CO)₄] (**2**). Thermal ellipsoids are drawn at the 50% probability level, and hydrogen atoms are omitted for clarity.

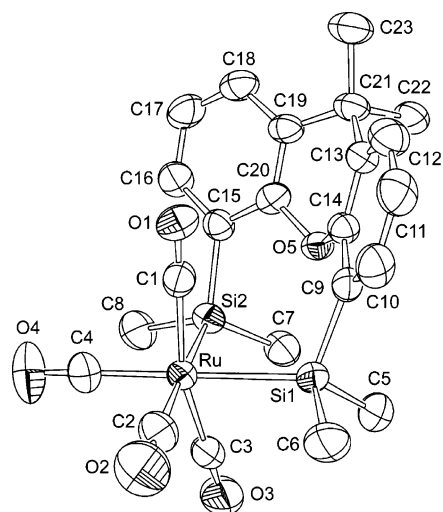


Figure 3. ORTEP drawing of *cis*-[Ru(xantsil)(CO)₄] (**3**). Thermal ellipsoids are drawn at the 50% probability level, and hydrogen atoms are omitted for clarity.

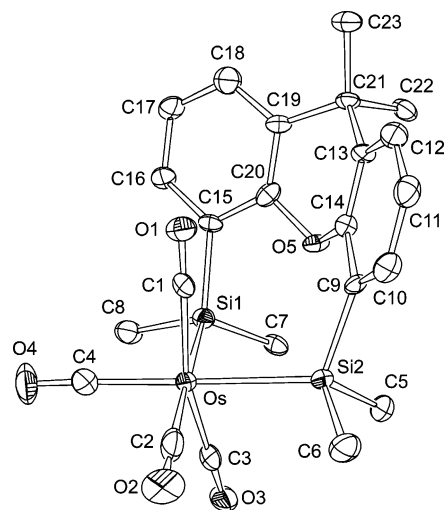


Figure 4. ORTEP drawing of *cis*-[Os(xantsil)(CO)₄] (**4**). Thermal ellipsoids are drawn at the 50% probability level, and hydrogen atoms are omitted for clarity.

the ideal 90° by the formation of the eight-membered chelate ring. The xanthene moiety is strongly bent, with a dihedral angle of 43° between the least-square planes of the two aromatic rings in the xantsil ligand. This is in contrast to the near-planar arrangement of the xanthene core in the ligand precursor **1b**, demonstrating the flexibility of the xantsil ligand. The two axial CO ligands are bent slightly toward the electron-releasing xantsil ligand, as evidenced by the C1–M–C3 angles (158.8(3)–162.8(2)°), which are far from linear. Distortion from the octahedron to a bicapped tetrahedron has been discussed in several previous studies (Chart 2).^{11–13} Narrowing the trans L–M–L angle from 180° and widening the cis L–M–L angle leads to distortion of the octahedron (**A**) to a bicapped tetrahedron (**B**). Hoffmann et al. showed by extended Hückel calculations that σ -donors prefer position D of the capping ligand in the bicapped tetrahedron **C**, while σ -acceptors prefer position A.^{11a} Complexes **2–4** approach the pseudo-bicapped tetrahedron, with the two silyl groups of xantsil as σ -donors.

The most characteristic feature in the structures of **2–4** is the exceptionally long metal–silicon bonds. These metal–silicon bonds are the longest of such bonds reported in the Cambridge Data Base (Fe–Si, 2.154–2.488 Å; Ru–Si, 2.177–2.539 Å; Os–Si, 2.254–2.517 Å). The lengthening is attributable to the special steric requirement of the xantsil ligand on coordination to the metal center (Table 1). On $\kappa^2\text{Si}_2\text{Si}$ -coordination, the xantsil ligand fixes two methyl groups C5 and C7 at an extremely short interatomic distance (3.469(13)–3.490(9) Å) compared to the sum of the effective van der Waals radii of the two methyl groups (4.0 Å). The steric repulsion between these methyl groups forces the other two methyl groups (C6 and C8) to move toward the carbonyl ligands. The observed interatomic distances between C6 and O2 and between C8 and O4 (3.203(12)–3.349(10) Å) are significantly shorter than the sum of the van der Waals radii of the methyl group and oxygen atom (3.4 Å), leading to considerable stretching of the metal–silicon bonds.

(10) Krentz, R.; Pomeroy, R. K. *Inorg. Chem.* **1985**, *24*, 2976.

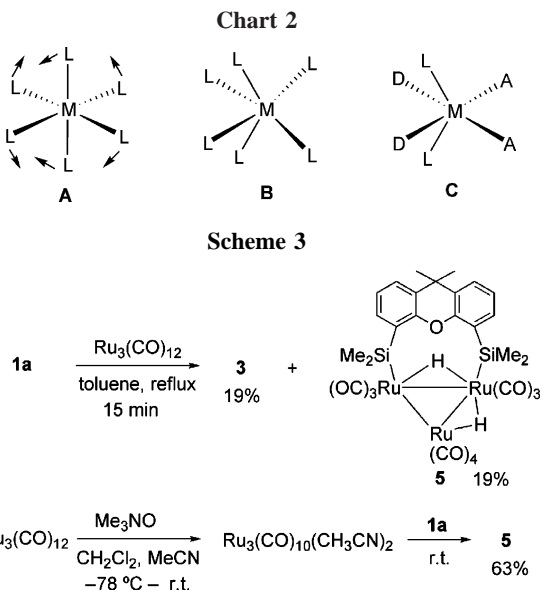
(11) (a) Hoffmann, R.; Howell, J. M.; Rossi, A. R. *J. Am. Chem. Soc.* **1976**, *98*, 2484. (b) Kubacek, P.; Hoffmann, R. *J. Am. Chem. Soc.* **1981**, *103*, 4320.

(12) Templeton, J. L.; Winston, P. B.; Ward, B. C. *J. Am. Chem. Soc.* **1981**, *103*, 7713.

(13) Kamata, M.; Hirotsu, K.; Higuchi, T.; Tatsumi, K.; Hoffmann, R.; Yoshida, T.; Otsuka, S. *J. Am. Chem. Soc.* **1981**, *103*, 5772.

Table 1. Summary of Selected Interatomic Distances and Angles for *cis*-[M(xantsil)(CO)₄] (M = Fe (2), Ru(3), Os(4))

	2	3	4
Selected Interatomic Distances (Å)			
M–Si1, M–Si2	2.497(3), 2.489(3)	2.562(2), 2.564(2)	2.5750(18), 2.5689(18)
Si1...Si2, C5...C7	3.747(2), 3.469(13)	3.786(2), 3.490(9)	3.790(2), 3.479(10)
C6...O2, C8...O4	3.203(12), 3.231(13)	3.320(9), 3.349(10)	3.274(10), 3.348(9)
Selected Interatomic Angles (deg)			
Si1–M–Si2, Si1–M–C1	97.45(8), 84.0(2)	95.26(6), 84.5(2)	94.90(6), 83.76(19)
Si1–M–C2, Si1–M–C3	85.8(3), 83.4(3)	85.8(2), 85.4(2)	85.2(2), 86.6(2)
Si1–M–C4, Si2–M–C1	176.6(3), 87.3(2)	178.5(2), 88.2(2)	178.5(2), 87.28(18)
Si2–M–C2, Si2–M–C3	173.9(3), 77.6(3)	174.9(2), 78.9(2)	174.8(2), 78.3(2)
Si2–M–C4, C1–M–C2	85.9(3), 98.2(4)	85.8(2), 96.8(3)	85.6(2), 97.9(3)
C1–M–C3, C1–M–C4	158.8(3), 96.1(3)	162.8(2), 94.4(3)	161.9(3), 94.8(3)
C2–M–C3, C2–M–C4	97.8(4), 90.9(4)	96.3(3), 93.2(3)	96.5(3), 94.4(3)
C3–M–C4	97.5(4)	95.9(3)	95.0(3)
Dihedral Angles between Two Aromatic Rings in Xantsil (deg)			
	43.4(3)	43.3(2)	43.3(2)



Ru(=CHPh)Cl₂(xantphos) has been reported to have a bite angle of 161°, indicative of the *trans* configuration of two phosphine parts in xantphos.¹⁴ Silyl groups in xantsil, however, are expected to exhibit the exceptional electron-releasing and *trans* influencing character. Such features would prevent the *trans*-configuration of two silyl groups in xantsil.¹⁵

The synthetic study of **3** revealed the formation of a trinuclear ruthenium cluster [Ru₃(xantsil)(μ-H)₂(CO)₁₀] (**5**), which was obtained by the direct reaction of [Ru₃(CO)₁₂] with **1a** in refluxing toluene for 15 min and by the reaction of [Ru₃(CO)₁₀(CH₃CN)₂] with **1a** at room temperature (Scheme 3). In the direct reaction of [Ru₃(CO)₁₂], the trinuclear complex **5** was formed in 19% yield together with the mononuclear complex **3** (19%) and unreacted [Ru₃(CO)₁₂]. The isolation of **5** by silica gel flash chromatography was not successful because of the decomposition of **5**. Recrystallization of the crude product from toluene afforded colorless crystals of **3** along with large red crystals identified as aggregates of **3** and **5** at a 1:1 ratio. The synthesis of **5** via [Ru₃(CO)₁₀(NCMe)₂] afforded reddish-orange crystals of **5** in 63% yield.

(14) Nieczypor, P.; van Leeuwen, P. W. N. M.; Mol, J. C.; Lutz, M.; Spek, A. L. *J. Organomet. Chem.* **2001**, 625, 58.

(15) The X-ray characterized *trans*-bis(silyl) complexes are very limited: (a) Shimada, S.; Tanaka, M.; Honda, K. *J. Am. Chem. Soc.* **1995**, 117, 8289. (b) Kim, Y.-J.; Park, J.-I.; Lee, S.-C.; Osakada, K.; Tanabe, M.; Choi, J.-C.; Koizumi, T.; Yamamoto, T. *Organometallics* **1999**, 18, 1349. (c) Wu, Z.; Diminnie, J. B.; Xue, Z. *J. Am. Chem. Soc.* **1999**, 121, 4300. (d) Qiu, H.; Cai, H.; Woods, J. B.; Wu, Z.; Chen, T.; Yu, X.; Xue, Z.-L. *Organometallics* **2005**, 24, 4190.

A direct reaction between [Ru₃(CO)₁₂] and a bis(hydrosilyl) ligand precursor has been reported in the preparation of [Ru₃(μ-SiMe₂C₅H₄FeC₅H₄SiMe₂(μ-H)₂(CO)₁₀].¹⁶ Unlike the xantsil complexes, however, the reaction of [Ru₃(CO)₁₂] with this 1,1'-bis(dimethylsilyl)ferrocene ligand precursor was found to be highly dependent on the ratio of the reactants. A 3:1 molar ratio of [Ru₃(CO)₁₂] to the ligand precursor was required to obtain the mononuclear complex *cis*-[Ru(κ²Si, Si-SiMe₂C₅H₄FeC₅H₄-SiMe₂)(CO)₄], while an equimolar ratio of reactants gave the trinuclear cluster exclusively.

Synthesis using labile trinuclear ruthenium clusters has also been reported as part of the preparation of other silyl trinuclear clusters such as [Ru₃(SiR₃)₂(μ-H)₂(μ-C₄H₄N₂)(CO)₈] (R = Et, Ph) through the reaction of the activated [Ru₃(μ-C₄H₄N₂)(μ-CO)₃(CO)₇] with tertiary silanes in refluxing THF.¹⁷ Because of the high lability of acetonitrile ligands, [Ru₃(CO)₁₀(NCMe)₂] is convenient for the synthesis of **5** without heating.

An ORTEP drawing of the 1:1 aggregate of [Ru(xantsil)(CO)₄] (**3**) and [Ru₃(xantsil)(μ-H)₂(CO)₁₀] (**5**) is shown in Figure 5. There is no significant interaction between the two molecules. The structural features of fragment **3** are essentially the same as those observed for **3** alone. The ORTEP drawing of fragment **5** and selected interatomic distances and angles are shown in Figure 6. The three ruthenium atoms form a triangle with xantsil as a bridging ligand between Ru2 and Ru3. The Ru–Ru bonds (2.94–3.16 Å) are considerably longer than those of Ru₃(CO)₁₂ (2.854 Å)¹⁸ and are comparable to those of the related Ru₃ clusters.^{16,19} The silyl groups are bound to the ruthenium atoms in the plane of a Ru₃ triangle. All carbonyl ligands are terminal. The xanthene moiety is close to planar, exhibiting a dihedral angle of 7.7(1)° between the least-square planes of two aromatic rings in xantsil. The Ru2–Si4 and Ru3–Si3 bond lengths are consistent with the standard equilibrium bond length. Although the two bridging hydrogen atoms could not be located crystallographically, their existence is suggested by the NMR spectroscopic data (*vide infra*). These are assigned to the bridging positions between the two longest Ru–Ru bonds; Ru2–Ru3 (3.0123(3) Å) and Ru2–Ru4 (3.1600(3) Å), consistent with several reports on the elongation of Ru–Ru bonds when bridged by a hydrogen atom.^{17,19,20} Moreover, there is a

(16) Kotani, S.; Tanizawa, T.; Adachi, T.; Yoshida, T.; Sonogashira, K. *Chem. Lett.* **1994**, 1665.

(17) Cabeza, J. A.; Franco, R. J.; Llamazares, A.; Riera, V.; Bois, C.; Jeannin, Y. *Inorg. Chem.* **1993**, 32, 4640.

(18) (a) Mason, R.; Rae, A. I. M. *J. Chem. Soc. A* **1968**, 778. (b) Churchill, M. R.; Hollander, F. J.; Hutchinson, J. P. *Inorg. Chem.* **1977**, 16, 2655.

(19) Klein, H.-P.; Thewalt, U.; Herrmann, G.; Süß-Fink, G.; Moinet, C. *J. Organomet. Chem.* **1985**, 286, 225.

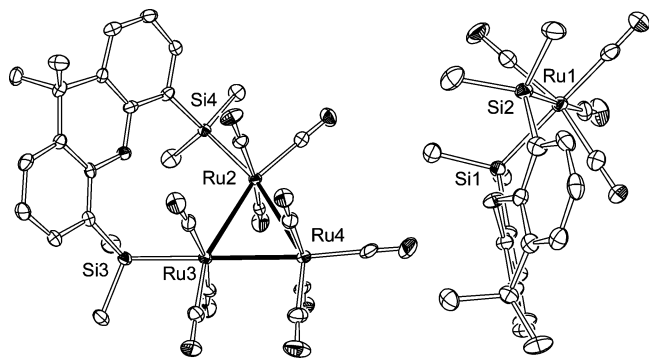


Figure 5. ORTEP drawing of the 1:1 aggregate of *cis*-[Ru(xantsil)(CO)₄] (**3**) and [Ru₃(xantsil)(μ-H)₂(CO)₁₀] (**5**) at the 50% probability level. Hydrogen atoms are omitted for clarity.

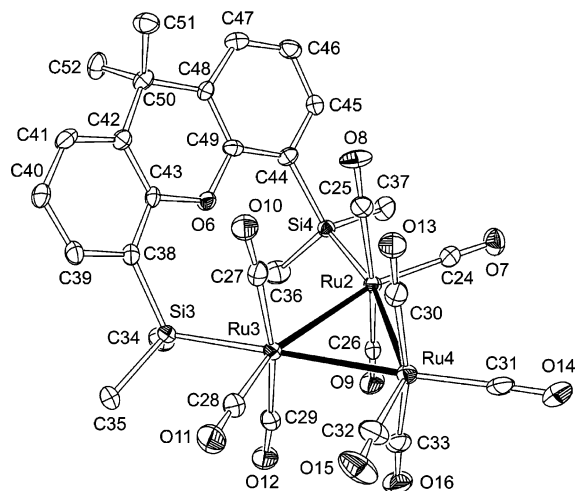
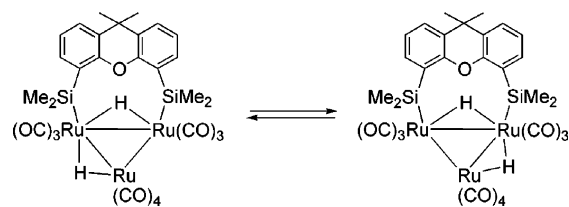


Figure 6. ORTEP drawing of the [Ru₃(xantsil)(μ-H)₂(CO)₁₀] (**5**) fragment at the 50% probability level. Selected interatomic distances (Å) and angles (deg): Ru2–Ru3, 3.0123(3); Ru3–Ru4, 2.9378(4); Ru2–Ru4, 3.1600(3); Ru2–Si4, 2.4854(8); Ru3–Si3, 2.4479(9); C24···C31, 4.433(5); C28···C32, 2.998(5); Ru2–Ru3–Ru4, 64.144(8); Ru3–Ru4–Ru2, 59.073(8); Ru4–Ru2–Ru3, 56.783(8).

large difference between the interatomic distances of C24···C31 (4.433(5) Å) and C28···C32 (2.998(5) Å), clearly indicating the presence of a hydrogen atom bridging the Ru2–Ru4 bond and the absence of such a bridging atom on Ru3–Ru4. The steric requirement for the bridging hydrogen atom increases the distance between carbonyl ligands C24–O7 and C31–O14, whereas the C28–O11 to C32–O15 distance is unaffected.

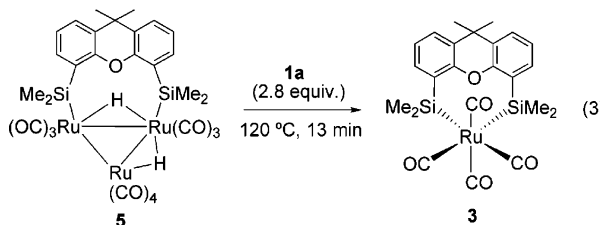
The appearance of several bands in the 1986–2116 cm⁻¹ region of the IR spectrum indicates that all carbonyl ligands are terminal. The ¹H NMR spectrum of **5** exhibits singlet signals at δ -16.27 and -14.94, indicating the presence of two chemically inequivalent bridging hydrido ligands. The dynamic behavior of **5** was examined in toluene-*d*₈ by variable temperature ¹H NMR study. At 295 K, the two singlets for the methyl groups in SiMe₂ and other two singlets for those in 9,9-CMe₂ appear as broad signals. On lowering the temperature, these signals become sharp. On increasing the temperature, each of them coalesces and finally becomes a sharp singlet. The coalescence point for the 9,9-CMe₂ moiety could not be determined owing to overlap with other signals. From the data for the exchange of SiMe₂ groups (Δ*ν* (at 215 K) = 17.6 Hz,

Scheme 4

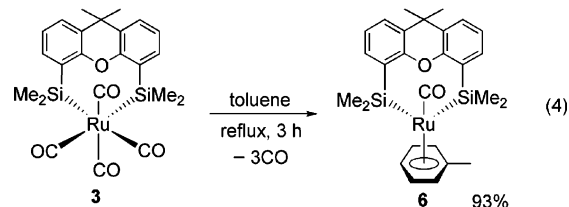


$T_c = 307$ K), the barrier at 307 K is calculated by the coalescence point method to be $\Delta G_{307}^\ddagger = 68$ kJ mol⁻¹. This dynamic process is also likely to include the inversion of the puckered chelate ring as proposed for the dynamic behavior of **2**, **3**, and **4**. Moreover, the ²⁹Si{¹H} NMR spectrum displays one resonance at δ 7.2. Another dynamic process of **5**, yielding two equivalent Ru(CO)₃(SiMe₂) moieties, is thus considered to be too fast to be detected by NMR spectroscopy (Scheme 4).

The possibility of **5** as an intermediate leading to the formation of **3** was further investigated by monitoring the thermal reaction of **5** with **1a** (2.8 equiv) by ¹H NMR spectroscopy. Thermolysis at 120 °C for 13 min was sufficient to achieve complete consumption of **5** to give **3** in 28% yield based on the number of carbonyl ligands (eq 3). As thermolysis of **5** in the absence of **1a** did not give **3**, the path leading to **3** starts from **5** and **1a**.



Consistent with the general stability of organometallic complexes, the xantsil-iron complex **2** was unstable and thus difficult to handle as a starting material, while the xantsil-osmium complex **4** was too stable to allow further transformation reactions. The xantsil-ruthenium complex **3** exhibits moderate reactivity: The thermal reaction of **3** in refluxing toluene for 3 h resulted in the replacement of three carbonyl ligands with toluene to give [Ru(xantsil)(CO)(η⁶-toluene)] (**6**) in 93% yield (eq 4). Complex **6** was uniquely characterized by NMR and X-ray diffraction data (Figure 7).⁹



In contrast to **3**, no analogous replacement of CO was detected for bis(silyl)ruthenium(II) complex **7** upon treatment in toluene-*d*₈ at 130 °C for 2 days (eq 5), implying that the xantsil ancillary ligand is crucial in the substitution reaction of three CO groups with arene. A plausible mechanism involves the initial formation of [Ru(κ³-Si₂Si₁-O-xantsil)(CO)₃] through the dissociation of one carbonyl ligand, followed by the intramolecular coordination of the xanthene oxygen atom. Dissociation of the carbonyl ligand would be enhanced by the severe steric repulsion between the SiMe₂ moiety and the three *fac*-carbonyl ligands and/or pre-coordination of the xanthene oxygen atom to lower the activation barrier. The incoming toluene interacts with the coordinatively

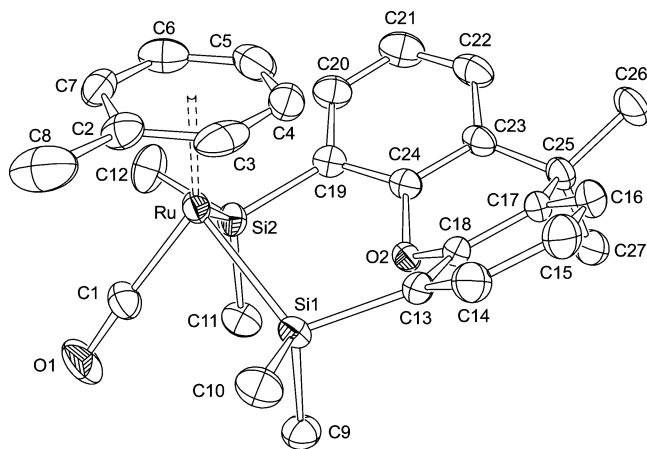
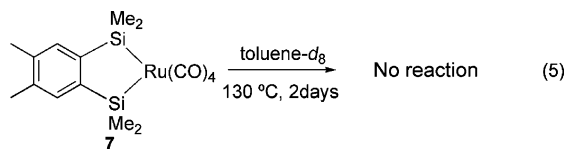


Figure 7. ORTEP drawing of $[\text{Ru}(\text{xantsil})(\eta^6\text{-toluene})(\text{CO})]$ (**6**) at the 50% probability level. Selected interatomic distances (Å) and angles (deg): Ru–Si1, 2.422(2); Ru–Si2, 2.420(2); Ru–C1, 1.815(6); Ru–C2, 2.327(5); Ru–C3, 2.294(6); Ru–C4, 2.287(6); Ru–C5, 2.320(6); Ru–C6, 2.334(6); Ru–C7, 2.314(5); Si1–Ru–Si2, 94.81(6).

unsaturated Ru(II) species derived from the facile dissociation of the xanthene oxygen atom and finally replaces with three carbonyl ligands to give **6**. A xanthene-based diphosphine ligand has been known to function as a κ^3P,P,O -terdentate ligand toward transition metals.^{5e,21}



Conclusion

Group-8 transition-metal mononuclear carbonyl complexes supported by the bis(silyl) ligand (xantsil) were successfully prepared by reactions between the appropriate metal carbonyls and xantsil- H_2 (**1a**) under thermal or photochemical conditions. A Ru_3 cluster with xantsil was also synthesized from $\text{Ru}_3(\text{CO})_{12}$ or $\text{Ru}_3(\text{CO})_{10}(\text{CH}_3\text{CN})_2$. Spectroscopic and X-ray diffraction analyses show that the eight-membered chelate ring of xantsil induces steric crowding among the SiMe_2 groups and the three fac-carbonyl ligands, resulting in unusually long M–Si bonds and facile replacement of three carbonyl ligands with arene. The electronic effect of the strongly σ -donating silyl groups in xantsil is proposed as the cause of distortion from the expected octahedron to the bicapped-tetrahedron. The steric requirement and electronic effect of xantsil may be applicable in the development of new types of metal-mediated catalytic reactions. In $[\text{Ru}_3(\text{xantsil})(\mu\text{-H})_2(\text{CO})_{10}]$ (**5**), xantsil serves as a bridging ligand to a Ru–Ru bond of the Ru_3 triangle and is likely to help prevent fragmentation. The preparation of the trinuclear ruthenium cluster is particularly significant since $\text{Ru}_3(\text{CO})_{12}$ and its derivatives are frequently involved in metal-catalyzed transformation reactions.

Experimental Section

General. All manipulations were performed under an inert atmosphere of dry argon or nitrogen or under high vacuum. Diethyl ether, hexane, and toluene were distilled from sodium-benzophenone ketyl, and dichloromethane was distilled from CaH_2 . Benzene- d_6 and cyclohexane- d_{12} were dried over activated 4 Å molecular sieves or over a potassium mirror and transferred to an NMR tube under

vacuum for the sealed-tube reactions. 9,9-Dimethylxanthene,²² 2,7-di-*t*-butyl-9,9-dimethylxanthene,²³ $[\text{Ru}_3(\text{CO})_{12}]$,²⁴ and $[\text{Os}_3(\text{CO})_{12}]$ ²⁵ were prepared according to literature methods. Tetracarbonyl{4,5-dimethylphenylene-1,2-bis(dimethylsilyl)}ruthenium (**7**) was synthesized by the synthetic procedure for tetracarbonyl{phenylene-1,2-bis(dimethylsilyl)}ruthenium.²⁶ Other reagents were purchased from commercial sources and used without further purification. NMR measurements were performed on a Bruker ARX-300 or AVANCE-300 NMR spectrometer at room temperature unless otherwise stated. ^1H NMR spectra were referenced to $\text{Si}(\text{CH}_3)_4$ through the residual peaks of the employed solvents, $^{13}\text{C}\{^1\text{H}\}$ and $^{29}\text{Si}\{^1\text{H}\}$ NMR spectra were referenced to external $\text{Si}(\text{CH}_3)_4$ at δ 0.0, and ^{31}P NMR spectra were referenced to external 85% H_3PO_4 at δ 0.0. IR spectra were obtained on a Horiba FT-200 or FT-730 spectrophotometer. Mass spectra were measured on a JEOL HX110 or Hitachi M-2500S mass spectrometer.

4,5-Bis(dimethylsilyl)-9,9-dimethylxanthene (1a). To a mixture of 9,9-dimethylxanthene (14.0 g, 66.6 mmol), TMEDA (21.3 mL, 133 mmol) in diethyl ether (270 mL), and hexane (200 mL) was added a solution of *n*-BuLi (108 mL of 1.48 M solution in hexane, 160 mmol) diluted with hexane (200 mL) in a dropwise manner over a period of 1 h. The mixture was then heated to 40 °C for 3 h, causing the solution to become deep red in color. After cooling the solution to 0 °C, HSiMe_2Cl (15.1 g, 160 mmol) in hexane (130 mL) was added to the solution over a period of 90 min under constant stirring, causing the solution to become deep red to yellow in color. After further stirring the solution at room temperature for 30 min, the reaction mixture was placed in a separatory funnel and washed with distilled water. The organic layer was dried over magnesium sulfate, and the volatiles were removed under vacuum. Purification of the viscous yellow residue by flash chromatography (silica gel, hexane) followed by recrystallization from hot hexane gave colorless crystals of **1a**. Yield: 20.9 g (96%). ^1H NMR (300 MHz, benzene- d_6): δ 0.43 (d, $^3J = 3.5$ Hz, 12H, SiMe_2), 1.42 (s, 6H, 9-Me), 5.15 (septet, $^3J = 3.5$ Hz, 2H, SiH), 6.99 (t, $^3J = 7.5$ Hz, 2H, xantsil 2,7-H), 7.24 (dd, $^3J = 1.7$, $^4J = 7.4$ Hz, 2H, xantsil 1,8-H or 3,6-H), 7.32 (dd, $^3J = 1.7$, $^4J = 7.4$ Hz, 2H, xantsil 1,8-H or 3,6-H). $^{13}\text{C}\{^1\text{H}\}$ NMR (75.5 MHz, benzene- d_6): δ -3.3 (SiMe_2), 32.8 (9-Me), 34.2 (9-C), 123.4, 124.7, 128.4, 129.4, 133.8, 155.1 (aromatic carbons). $^{29}\text{Si}\{^1\text{H}\}$ NMR (59.6 MHz, benzene- d_6): δ -22.2. IR (hexane, cm^{-1}): 2119 (m) (ν_{SiH}), 2158s (ν_{SiH}). Mass (FAB, Xe, *m*-nitrobenzyl alcohol matrix) m/z 326 (M^+ , 5), 311 ($\text{M}^+ - \text{CH}_3$, 100). Anal. Calcd for $\text{C}_{19}\text{H}_{26}\text{OSi}_2$: C, 69.88; H, 8.02. Found: C, 70.02; H, 7.91.

4,5-Bis(dimethylsilyl)-2,7-di-*t*-butyl-9,9-dimethylxanthene (1b). A method similar to that for **1a** was employed for the preparation of colorless crystals of **1b** using *n*-BuLi (16.2 mL of 1.48 M solution in hexane, 24 mmol), 2,7-di-*t*-butylxanthene (3.22 g, 10.0 mmol), TMEDA (3.20 mL, 20.0 mmol), and HSiMe_2Cl (2.27 g, 24.0 mmol). Yield: 1.84 g (42%). ^1H NMR (300 MHz, benzene- d_6): δ 0.50 (d, $^3J = 3.7$ Hz, 12H, SiMe_2), 1.33 (s, 18H, tBu), 1.60 (s, 6H,

(21) (a) Sandee, A. J.; van der Veen, L. A.; Reek, J. N. H.; Kamer, P. C. J.; Lutz, M.; Spek, A. L.; van Leeuwen, P. W. N. *M. Angew. Chem., Int. Ed.* **1999**, *38*, 3231. (b) Zuideveld, M. A.; Swennenhuis, B. H. G.; Boele, M. D. K.; Guari, Y.; van Strijdonck, G. P. F.; Reek, J. N. H.; Kamer, P. C. J.; Goubitz, K.; Fraanje, J.; Lutz, M.; Spek, A. L.; van Leeuwen, P. W. N. *M. Dalton Trans.* **2002**, 2308.

(22) (a) Corey, E. J.; Chaykovsky, M. *J. Am. Chem. Soc.* **1965**, *87*, 1345. (b) Chanzan, J. B.; Ourisson, G. *Bull. Soc. Chim. Fr.* **1968**, *4*, 1384. (c) Bavin, P. M. G. *Can. J. Chem.* **1960**, *38*, 882.

(23) Nowick, J. S.; Ballester, P.; Ebmeyer, F.; Rebek, J., Jr. *J. Am. Chem. Soc.* **1990**, *112*, 8902.

(24) (a) Eady, C. R.; Jackson, P. F.; Johnson, B. F. G.; Lewis, J.; Malatesta, M. C.; Mcpartlin, M.; Nelson, W. J. *H. J. Chem. Soc., Dalton Trans.* **1980**, 383. (b) Bruce, M. I.; Jensen, C. M.; Jones, N. L.; *Inorg. Synth.* **1989**, *26*, 259.

(25) Gade, L. Z.; Johnson, B. F. G.; Lewis, J.; Loveday, P. A.; Herrmann, W. A., Eds. *Synthetic Methods of Organometallic and Inorganic Chemistry*; Thieme Medical Publishers: Stuttgart, Germany, 1987; 7, 28.

(26) Fink, W. *Helv. Chim. Acta* **1976**, *59*, 606.

9-Me₂), 5.21 (septet, ³J = 3.7 Hz, 2H, SiH), 7.54 (d, ⁴J = 2.3 Hz, 2H, 1,8-H or 3,6-H), 7.56 (d, ⁴J = 2.3 Hz, 2H, 3,6-H). ¹³C{¹H} NMR (75.5 MHz, benzene-*d*₆): δ -3.2 (SiMe₂), 31.7 (CMe₃), 33.3 (9,9-Me₂), 34.5, 34.8 (9-C, CMe₃), 124.1, 125.2, 128.7, 130.6, 153.3 (aromatic carbons). ²⁹Si{¹H} NMR (59.6 MHz, benzene-*d*₆): δ -21.3. IR (KBr, cm⁻¹): 2156 (s) (ν_{SiH}). Mass (EI, 70 eV) *m/z* 438 (M⁺, 10), 423 (M⁺ - CH₃, 100). Anal. Calcd for C₂₇H₄₂O₅Si₂: C, 73.90; H, 9.65. Found: C, 73.67; H, 9.68.

cis-[Fe(xantsil)(CO)₄] (2). A dichloromethane solution (1.5 mL) of Fe(CO)₅ (196 mg, 1.00 mmol) and **1a** (98 mg, 0.30 mmol) was irradiated under a medium-pressure Hg lamp (450 W) for 5 h. The insoluble Fe₂(CO)₉ byproduct was then removed by filtration, and the filtrate was concentrated and subjected to silica gel column chromatography. Complex **2** was eluted with a 3:1 mixture of hexane and diethyl ether. Evaporation of the eluent under reduced pressure gave colorless crystals of **2**. Yield: 79 mg (53%). ¹H NMR (300 MHz, benzene-*d*₆): δ 0.88 (s, 12H, SiMe₂), 1.42 (s, 6H, 9-Me₂), 7.04 (t, ³J = 7.5 Hz, 2H, xantsil 2,7-H), 7.22 (br. d, 2H, ³J = 7.5 Hz, 2H, xantsil 1,8-H or 3,6-H), 7.25 (br. d, 2H, ³J = 7.5 Hz, 2H, xantsil 1,8-H or 3,6-H). ¹³C{¹H} NMR (75.5 MHz, benzene-*d*₆): δ 6.9 (SiMe₂), 27.0 (9,9-CMe₂), 36.3 (9,9-CMe₂), 124.1, 126.0, 131.1, 131.2, 133.6, 158.3 (aromatic carbons), 206.6, 208.4 (CO). ²⁹Si{¹H} NMR (C₆D₆): δ 9.0. IR (KBr, cm⁻¹): 1981 (s), 1994 (s), 2011 (s), 2069 (s) (ν_{CO}). Mass (FAB, Xe, *m*-nitrobenzyl alcohol matrix) *m/z* 493 (M⁺ + 1, 4), 478 (M⁺ - Me + 1, 12), 464 (M⁺ - CO, 12), 436 (M⁺ - 2CO, 11), 408 (M⁺ - 3CO, 100), 380 (M⁺ - 4CO, 66). Anal. Calcd for C₂₃H₂₄O₅Si₂Fe: C, 56.10; H, 4.91. Found: C, 55.85; H, 5.18.

cis-[Ru(xantsil)(CO)₄] (3). Ru₃(CO)₁₂ (1.00 g, 1.56 mmol) and **1a** (1.23 g, 3.77 mmol) were dissolved in toluene (200 mL) and the solution heated to 120 °C. After 90 min, the initial red color of the solution changed to dark brown, and the thin-layer chromatographic (TLC) spot of **1a** disappeared. Removal of volatiles under vacuum gave a dark brown residue which was subjected to flash chromatography (silica gel, hexane/toluene = 3:1) to give a mixture of **3** and Ru₃(CO)₁₂ (1.00 g) as the first fraction and a mixture of **1a** and an unidentified brown product (0.40 g) as the second fraction. Recrystallization of the former from hot hexane afforded pure **3** as colorless crystals. Yield: 700 mg (34%). ¹H NMR (300 MHz, benzene-*d*₆): δ 0.88 (s, 12H, SiMe₂), 1.45 (s, 6H, 9,9-Me₂), 7.08 (t, ³J = 7.3 Hz, 2H, xantsil 2,7-H), 7.24 (dd, ⁴J = 1.4, ³J = 7.3 Hz, 2H, xantsil 1,8-H or 3,6-H), 7.32 (dd, ⁴J = 1.4, ³J = 7.3 Hz, 2H, xantsil 1,8-H or 3,6-H). ¹³C{¹H} NMR (75.5 MHz, benzene-*d*₆): δ 7.0 (SiMe₂), 27.3 (9-Me), 36.1 (C-Me₂), 123.8, 125.5, 131.0, 131.8, 133.3, 158.1 (aromatic carbons), 190.7, 197.7 (CO). ²⁹Si{¹H} NMR (59.6 MHz, benzene-*d*₆): δ -8.2. IR (hexane, cm⁻¹): 2015 (s), 2033 (s), 2042 (s), 2098 (s) (ν_{CO}). Mass (EI, 70 eV) *m/z* 538 (M⁺, 3), 510 (M⁺ - CO, 39), 482 (M⁺ - 2CO, 14), 454 (M⁺ - 3CO, 100). Anal. Calcd for C₂₃H₂₄O₅Si₂Ru: C, 51.38; H, 4.50. Found: C, 51.48; H, 4.47.

cis-[Os(xantsil)(CO)₄] (4). A toluene (6.0 mL) solution of Os₃(CO)₁₂ (75 mg, 0.083 mmol) and **1a** (95 mg, 0.29 mmol) was heated at 125 °C for 1 day. After cooling to room temperature, volatiles were removed under vacuum. Purification of the brown residue by silica gel flash chromatography with hexane/toluene eluent (hexane/toluene = 3:1) and subsequent recrystallization from hot hexane and toluene (4:1) gave **4** as colorless crystals. Yield: 45 mg (87%). ¹H NMR (300 MHz, benzene-*d*₆): δ 0.95 (s, 12H, SiMe₂), 1.45 (s, 6H, 9,9-Me₂), 7.06 (t, ³J = 7.4 Hz, 2H, xantsil 2,7-H), 7.21 (dd, ⁴J = 1.4, ³J = 7.4 Hz, 2H, xantsil 1,8-H or 3,6-H), 7.26 (dd, ⁴J = 1.4, ³J = 7.4 Hz, 2H, xantsil 1,8-H or 3,6-H). ¹³C{¹H} NMR (300 MHz, benzene-*d*₆): δ 5.9 (SiMe₂), 27.3 (9-CMe₂), 36.0 (9-CMe₂), 123.8, 125.5, 130.0, 131.4, 133.0, 158.3 (aromatic carbons), 171.2, 180.6 (CO). ²⁹Si{¹H} NMR (300 MHz, benzene-*d*₆): δ -31.7. IR (KBr, cm⁻¹): 1982 (br), 2008 (vs), 2038 (vs), 2100 (vs) (ν_{CO}). Mass (EI, 70 eV) *m/z* 628 (M⁺, 23), 613 (M⁺ - Me, 41), 600 (M⁺ - CO, 23), 585 (M⁺ - CO - Me, 10), 572 (M⁺ - 2CO, 11), 557 (M⁺ -

2CO - Me, 14), 544 (M⁺ - 3CO, 23), 528 (M⁺ - 3CO - Me - H, 100). Exact MS (70 eV, DEI) *m/z* calcd for C₂₃H₂₄O₅Si₂Os, 628.0777; found, 628.0756.

Preparation of [Ru₃(xantsil)(μ-H)₂(CO)₁₀] (5) from **1a and Ru₃(CO)₁₂.** Ru₃(CO)₁₂ (1.10 g, 1.72 mmol) and **1a** (1.69 g, 5.18 mmol) were dissolved in toluene (20 mL) and the solution was heated to 120 °C for 15 min. The resulting red reaction mixture was then allowed to cool to room temperature. Volatiles were removed under reduced pressure to give an orange oil, which was dissolved in toluene and stored at -78 °C for one week to give a mixture of small colorless crystals of **3** and large red crystals identified as a 1:1 aggregate of **3** and Ru₃(xantsil)(μ-H)₂(CO)₁₀ (**5**). The large crystals (0.92 g) containing **3** and **5** were separated manually from the finer crystals of **3** (0.25 g). Yield of **3**: 0.52 g (19%). Yield of **5**: 0.29 g (19%). Anal. Calcd for C₅₂H₅₀O₁₆Si₄Ru₄ (**3**:**5**): C, 43.15; H, 3.48. Found: C, 43.38; H, 3.74.

Preparation of [Ru₃(xantsil)(μ-H)₂(CO)₁₀] (5) from **1a and [Ru₃(CO)₁₀(NCMe)₂].** (a) To a dichloromethane (100 mL) solution of Ru₃(CO)₁₂ (0.100 g, 0.157 mmol) and **1a** (0.610 g, 1.87 mmol) cooled at -78 °C was added an acetonitrile (10 mL) solution of Me₃NO (38 mg, 0.051 mmol) in a dropwise manner. The reaction mixture was returned naturally to room temperature and then stirred for 4 h. The resulting orange solution was evaporated to dryness and the residue extracted with toluene (50 mL). The solvent was removed from the extract under vacuum, and the residue was further extracted with hexane (35 mL). Cooling of the concentrated solution to -48 °C gave reddish-orange crystals of **5**. Yield: 90 mg (63%). ¹H NMR (C₆D₆): δ -16.27, -14.94 (s, s, 1H, 1H, RuH), 0.97, 1.07 (s, s, 6H, 6H, SiMe₂), 1.42, 1.45 (s, s, 3H, 3H, 9,9-Me₂), 7.02 (t, ³J = 7.5 Hz, 2H, 2,7-H), 7.27, 7.49 (dd, dd, ⁴J = 1.6, ³J = 7.5 Hz, 4H, 1,3,6,8-H). ¹³C{¹H} NMR (C₆D₆): δ 9.1, 11.0 (SiMe₂), 32.4, 33.3, 34.2 (9-C, 9,9-Me₂), 123.4, 128.3, 130.0, 130.7, 132.6, 154.7 (aromatic carbons), 191.8, 201.5, 203.2 (CO). ²⁹Si{¹H} NMR (C₆D₁₂): δ 7.2. IR (KBr): 2116 (m), 2100 (w), 2085 (m), 2069 (w), 2056 (s), 2040 (s), 2025 (s), 2011 (w), 1998 (w), 1986 (w) (CO, cm⁻¹). Mass (FAB, Xe, *m*-nitrobenzyl alcohol matrix): *m/z* 911 (M⁺, 5), 827 (M⁺ - 3CO, 10), 399 (100).

Monitoring the Reaction of 5 and 1a. A Pyrex NMR tube was charged with **5** (1.0 mg, 1.1 μmol), **1a** (1.0 mg, 3.1 μmol), and Si(SiMe₃)₄ (internal standard) and connected to the vacuum line. Toluene-*d*₈ (0.5 mL) was introduced into the tube by the trap-to-trap transfer technique. The sample was then placed in an oil bath and heated to 120 °C, and the reaction was monitored by NMR spectroscopy.

[Ru(xantsil)(CO)(η⁶-C₆H₅CH₃)] (6). A solution of **3** (560 mg, 1.04 mmol) in toluene (140 mL) was refluxed in an oil bath at 120 °C for 3 h. After removal of the solvent, recrystallization of the residue from hot toluene afforded **6** as pale yellow crystals. Yield: 526 mg (93%). ¹H NMR (C₆D₁₂): δ 0.58, 0.63 (s, s, 6H, 6H, SiMe₂), 1.39, 1.82 (s, s, 3H, 3H, 9,9-Me₂), 1.77 (s, 3H, C₆H₅Me), 3.79 (t, ³J = 6.1 Hz, 1H, toluene *p*-H), 4.87 (t, ³J = 6.1 Hz, 2H, toluene *m*-H), 5.45 (d, ³J = 6.1 Hz, 2H, toluene *o*-H), 6.99 (t, ³J = 7.3 Hz, 2H, xantsil 2,7-H), 7.22, 7.24 (dd, dd, ⁴J = 1.4, ³J = 7.3 Hz, 4H, xantsil 1,3,6,8-H). ¹³C{¹H} NMR (C₆D₁₂): δ 4.4, 9.5, 20.4, 23.1, 31.0, 37.0 (alkyl C), 94.3, 97.6, 100.1, 109.9 (C₆H₅Me), 123.0, 123.8, 129.6, 134.6, 139.0, 159.4 (xanthene), 201.0 (CO). ²⁹Si{¹H} NMR (C₆D₁₂): δ 12.6. IR (KBr): 1913 (vs, CO) 1386 (s) cm⁻¹. Mass (EI, 70 eV) *m/z* 546 (M⁺, 65), 454 (M⁺ - C₆H₅Me, 100). Anal. Calcd for C₂₇H₃₂O₂Si₂Ru: C, 59.42; H, 5.91. Found: C, 59.48; H, 5.81.

Attempted Reaction of 7 with Toluene-*d*₈. Toluene-*d*₈ (0.3 mL) was transferred by the trap-to-trap method to an NMR tube containing **7** (5.0 mg, 12 μmol) under high vacuum and the tube flame-sealed. The tube was heated to 130 °C in an oil bath. The reaction was observed periodically by measurement of the ¹H NMR

Table 2. Crystallographic Data of 1b, 4, and 3·5

	1b	4	3·5
formula	C ₂₇ H ₄₂ OSi ₂	C ₂₃ H ₂₄ O ₅ OsSi ₂	C ₅₂ H ₄₈ O ₁₆ Ru ₄ Si ₄
fw	438.79	626.80	1445.54
cryst size (mm ³)	0.20 × 0.20 × 0.20	0.35 × 0.30 × 0.10	0.30 × 0.10 × 0.10
cryst color, habit	colorless prismatic	colorless block	red block
cryst syst	monoclinic	monoclinic	triclinic
space group	<i>P2</i> ₁	<i>P2</i> ₁ / <i>n</i>	<i>P</i> $\bar{1}$
<i>a</i> (Å)	10.319(4)	12.3110(7)	15.2588(9)
<i>b</i> (Å)	10.579(3)	10.0336(6)	17.104(1)
<i>c</i> (Å)	13.042(3)	19.1542(19)	12.2358(6)
α (deg)			90.324(2)
β (deg)	97.83(2)	93.018(4)	111.541(2)
γ (deg)			103.163(3)
<i>V</i> (Å ³)	1410.5(8)	2362.7(3)	2878.2(3)
<i>Z</i>	2	4	2
<i>F</i> ₀₀₀	480	1224	1440
μ (Mo K α) (mm ⁻¹)	0.140	5.530	1.178
full matrix least-square	<i>F</i> ²	<i>F</i> ²	<i>F</i> ²
reflns collected	3603	18006	25453
independent reflns (<i>R</i> _{int})	3420 (0.0281)	5019 (0.0282)	12542 (0.0384)
abs corr	empirical	numerical	numerical
max and minimum transmission	0.57 and 1.00	0.25 and 0.61	0.72 and 0.89
no. variables	353	286	697
<i>R</i> ₁ , <i>wR</i> ₂ (all data)	0.1032, 0.1597	0.0356, 0.1056	0.0389, 0.0947
<i>R</i> ₁ , <i>wR</i> ₂ [<i>I</i> > 2 σ (<i>I</i>)]	0.0542, 0.1355	0.0290, 0.0830	0.0314, 0.0898
GOF	1.01	1.182	1.041
largest difference peak and hole (e ⁻ Å ⁻³)	0.29 and -0.28	1.152 and -2.494	0.861 and -0.743

spectra. No change was observed in the spectra over 2 days of heating.

X-ray Structure Determination of 1b, 4, and 3·5. Crystals of **1b**, **4**, and **3·5** were mounted at the end of a glass fiber for analysis using a Rigaku RAXIS-RAPID imaging plate diffractometer with graphite monochromated Mo K α radiation. Data were collected at 150 K to a maximum 2θ value of 55.0°. Empirical or numerical absorption correction was applied, and the data were corrected for Lorentz and polarization effects. The structure was solved by direct methods and refined by full matrix least-squares techniques on all *F*² data (SHELXL-97). The non-hydrogen atoms were refined anisotropically, and hydrogen atoms on the silicon atoms in **1b** were refined isotropically. Other hydrogen atoms were

Table 3. Crystallographic Data of 2, 3, and 6

	2	3	6
formula	C ₂₃ H ₂₄ FeO ₅ Si ₂	C ₂₃ H ₂₄ O ₅ RuSi ₂	C ₂₇ H ₃₂ O ₂ RuSi ₂
fw	492.46	537.68	545.79
cryst size (mm ³)	0.30 × 0.25 × 0.20	0.30 × 0.30 × 0.30	0.30 × 0.30 × 0.25
cryst color, habit	colorless prismatic	colorless prismatic	colorless prismatic
cryst syst	monoclinic	monoclinic	monoclinic
space group	<i>P2</i> ₁ / <i>n</i>	<i>P2</i> ₁ / <i>n</i>	<i>P2</i> ₁ / <i>n</i>
<i>a</i> (Å)	12.214(5)	12.372(5)	9.565(8)
<i>b</i> (Å)	10.05(1)	10.10(1)	14.535(9)
<i>c</i> (Å)	19.450(5)	19.524(5)	18.479(6)
β (deg)	92.87(3)	93.20(3)	92.26(4)
<i>V</i> (Å ³)	2385(2)	2436(2)	2567(2)
<i>Z</i>	4	4	4
<i>F</i> ₀₀₀	1024	1096	1128
μ (Mo K α) (mm ⁻¹)	0.763	0.772	0.725
full matrix least-square	<i>F</i>	<i>F</i>	<i>F</i>
reflns collected	6071	6188	6507
independent reflns (<i>R</i> _{int})	5807 (0.079)	5920 (0.035)	6150 (0.025)
no. data used ([<i>I</i> > 3 σ (<i>I</i>)]	2026	3112	3672
no. variables	280	280	289
<i>R</i> , <i>R</i> _w	0.0494, 0.0786	0.0409, 0.0558	0.0380, 0.0651
GOF	0.74	0.925	0.696
largest difference peak and hole (e ⁻ Å ⁻³)	0.36 and -0.24	0.43 and -0.51	0.59 and -0.34

located on the idealized positions. Selected crystallographic data are listed in Table 2.

X-ray Structure Determination of 2, 3, and 6. Crystals of **2**, **3**, and **6** were mounted at the end of a glass fiber for analysis using a Rigaku AFC-6S diffractometer with graphite monochromated Mo K α radiation. Data were collected at room temperature, using the ω - 2θ scan technique to maximum 2θ value of 55.0°. The data were corrected for Lorentz and polarization effects. The structure was solved by direct methods and expanded using Fourier techniques. Non-hydrogen atoms were refined anisotropically. Hydrogen atoms were included but not refined. Selected crystallographic data are listed in Table 3.

Supporting Information Available: CIF files giving X-ray crystallographic data for **1b**, **2**, **3**, **4**, **3·5**, and **6**. This material is available free of charge via the Internet at <http://pubs.acs.org>.

OM700720S